Published in final edited form as:
Anal Biochem. 2008 December 1; 383(1): . doi:10.1016/j.ab.2008.07.041.

Correlative and quantitative ^{1}H NMR-based metabolomics reveals specific metabolic pathway disturbances in diabetic rats

Shucha Zhang[a], **G.A. Nagana Gowda**[a], **Vincent Asiago**[a], **Narasimhamurthy Shanaiah**[a], **Coral Barbas**[b,*], and **Daniel Raftery**[a,*]

[a] Department of Chemistry, Purdue University, West Lafayette, IN 47907, USA

[b] San Pablo–CEU University, Boadilla del Monte, 28668 Madrid, Spain

Abstract

Type 1 diabetes was induced in Sprague–Dawley rats using streptozotocin. Rat urine samples (8 diabetic and 10 control) were analyzed by ^{1}H nuclear magnetic resonance (NMR) spectroscopy. The derived metabolites using univariate and multivariate statistical analysis were subjected to correlative analysis. Plasma metabolites were measured by a series of bioassays. A total of 17 urinary metabolites were identified in the ^{1}H NMR spectra and the loadings plots after principal components analysis. Diabetic rats showed significantly increased levels of glucose ($P < 0.00001$), alanine ($P < 0.0002$), lactate ($P < 0.05$), ethanol ($P < 0.05$), acetate ($P < 0.05$), and fumarate ($P < 0.05$) compared with controls. Plasma assays showed higher amounts of glucose, urea, triglycerides, and thiobarbituric acid-reacting substances in diabetic rats. Striking differences in the Pearson's correlation of the 17 NMR-detected metabolites were observed between control and diabetic rats. Detailed analysis of the altered metabolite levels and their correlations indicate a significant disturbance in the glucose metabolism and tricarboxylic acid (TCA) cycle and a contribution from gut microbial metabolism. Specific perturbed metabolic pathways include the glucose–alanine and Cori cycles, the acetate switch, and choline metabolism. Detection of the altered metabolic pathways and bacterial metabolites using this correlative and quantitative NMR-based metabolomics approach should help to further the understanding of diabetes-related mechanisms.

Keywords

Metabolomics; NMR spectroscopy; Type 1 diabetes; TCA cycle; Gluconeogenesis

Type 1 diabetes is an autoimmune disease resulting from the selective destruction of insulin-producing beta cells in the pancreatic islets [1]. It is growing in incidence and currently affects roughly 0.5% of the population in developed countries [2]. Despite the vast understanding of its epidemiology, a definite solution for the prevention of type 1 diabetes or its deleterious effects is still not forthcoming. Causes of diabetes are believed to be associated with genetics, environmental factors, nutritional effects, or a combination of these. Many experimental studies have used simulated diabetes on animal models to understand the molecular events associated with this disease and its complications [3,4]. Streptozotocin (STZ)[1] is well known to induce diabetogenic action by the selective

* Corresponding authors. Fax: +34 765 494 0239. (D. Raftery) cbarbas@ceu.es (C. Barbas), raftery@purdue.edu (D. Raftery)..

Appendix A. Supplementary data

Supplementary data associated with this article can be found, in the online version, at doi:10.1016/j.ab.2008.07.041.

destruction of pancreatic beta cells, and it is the most frequently used model for inducing diabetes mellitus [5–7]. The STZ-induced diabetic rat model provides a good platform to investigate diabetes using new approaches that may provide additional information on and insight into the mechanisms and effects of the disease.

The rapidly growing field of metabolomics (or metabonomics) that relates biological end points to multiple altered metabolite concentrations provides a wealth of biological information on complex systems [8–14]. It has been applied to a variety of diseases such as cancer [9,10], type 2 diabetes [4,15], and inborn errors of metabolism [16,17], and it has been used to study the effects of diet [18], drugs [19], toxins [20], and stress [21]. Metabolomics combines data-rich advanced analytical techniques such as nuclear magnetic resonance (NMR) spectroscopy and mass spectrometry with multivariate statistical analysis (MSA). NMR-based metabolomics is capable of simultaneously detecting a wide variety of extracellular (and intracellular in the case of tissue) metabolites that provide information on a large number of normal and abnormal biochemical pathways. To date, NMR spectroscopy has been applied to a number of diabetes studies [4,22–25]. NMR spectroscopy provides very high quantitative accuracy and reproducibility; is nondestructive, cost-effective, and rapid (typical requirements are a few minutes/sample); and requires limited or no sample preparation [26].

NMR data in combination with MSA allow the identification of potential biomarkers in biological specimens and an improved ability to identify specific metabolic pathways and networks associated with disease [1,17,18]. Widely used MSA methods such as principal component analysis (PCA) and partial least squares (PLS) discriminant analysis are applied for disease classification (through the use of scores plots) and biomarker detection (through the use of loadings plots) [27]. The computation of the correlation [28] among the detected metabolites can be used to study biological networks in metabolomics [17]; however, such approaches remain at a preliminary stage. In principle, the application of the correlation matrix is straightforward and holds a great deal of promise for tracing specific metabolic pathways to investigate metabolic disturbances due to disease or other effects.

This study aimed to identify disturbed metabolic pathways in STZ-induced diabetes using a ^{1}H NMR-based metabolomics approach. Absolute changes in the daily excreted quantities of detected metabolites (diabetic vs. control) and changes in the correlations among detected metabolites (for diabetic and control separately) were investigated. An integrated evaluation of metabolic changes in both quantities and correlations allowed us to trace specific disturbances in the metabolic pathways most associated with induced type 1 diabetes. We also compared our findings with current hypotheses regarding the detailed diabetes biochemistry.

Materials and methods

Materials

3-(Trimethylsilyl)propionic acid–d_4 sodium salt (TSP), α-tocopherol (all-rac), STZ, 2-thiobarbituric, D-(+)-glucose, ethanol, sodium pyruvate, sodium fumarate dibasic, allantoin, and sodium azide were obtained from Sigma (St. Louis, MO, USA) and were used without further purification.

[1]*Abbreviations used:* STZ, streptozotocin; NMR, nuclear magnetic resonance; MSA, multivariate statistical analysis; PCA, principal components analysis; PLS, partial least squares; TSP, 3-(trimethylsilyl)propionic acid–d_4 sodium salt; EDTA, ethylenediaminetetraacetic acid; TBARS, thiobarbituric acid-reacting substances; TCA, tricarboxylic acid; EGP, endogenous glucose production; CoA, coenzyme A; AceCS, acetyl–CoA synthetase; RBC, red blood cell.

Animals and samples

Female rats (Sprague–Dawley strain from the animal quarters located at San Pablo–CEU University), all similar in development stage (12 ± 2 weeks), were studied. The diabetic group (n = 8) consisted of animals that received an intraperitoneal dose (50 mg/kg) of STZ and showed glucose levels in the blood of more than 200 mg/dl after 4 days. The control group (n = 10) consisted of age- and gender-matched rats. Throughout the study, both diabetic and control animals were kept under appropriate conditions (22 ± 2 °C temperature and 55 ± 10% relative humidity). Air was replaced with adequate frequency, and the rats were maintained under a 12-h light–darkness cycle. Animals were housed in collective cages (1820 cm^3, not more than 6 animals per cage) with a bed of poplar shaving (29/12, Souralit, Spain), and all had free access to tap water and food (Harlan Global Diet 2014, Harlan Interfauna Ibérica, Madrid, Spain). Seven days after STZ administration, the rats were housed in metabolic cages and urine was collected and pooled every 8 h. Urine collection tubes contained hydrogen chloride (0.1 M) to avoid bacterial contamination. The total volume of urine for each rat excreted in 24 h was measured and stored at –80 °C. Urine samples were transported to Purdue University by air carrier over dry ice for metabolomics studies. On the day of sacrifice, animals were anesthetized with ketamine (75–100 mg/kg)/azepromacine (2.5 mg/ml) and blood was obtained by cardiac puncture in ethylenediaminetetraacetic acid (EDTA). The study was approved by the ethics committee of the San Pablo–CEU University (RD 223/1988) and is in agreement with Amsterdam Treaty and Spanish legislation.

Blood parameters

Plasma glucose, triglycerides, cholesterol, and urea were analyzed using commercial kits from Spinreact (Gerona, Spain). Thiobarbituric acid-reacting substances (TBARS) were measured according to Viana and coworkers [29].

^{1}H NMR spectroscopy

Frozen urine samples were thawed, and 500 μl was mixed with phosphate buffer (75 μl, 0.5 M, pH 7.0), D_2O (75 μl), TSP (5 μl in D_2O, 0.11 μmol), and sodium azide (5 μl in D_2O, 12.3 nmol). Resulting solutions were centrifuged to remove particulate matter, if any, and 500 μl of the supernatants was transferred to 5-mm NMR tubes. All ^{1}H NMR experiments were carried out at 25 °C on a Bruker DRX 500-MHz spectrometer equipped with an HCN ^{1}H inverse detection probe with triple axis magnetic field gradients. ^{1}H NMR spectra were acquired using the standard one-dimensional NOESY pulse sequence with water presaturation during the recycle delay of 3 s and a mixing time of 100 ms. Each dataset was averaged over 32 transients using 32,000 time domain points. The data were Fourier transformed after multiplying by an exponential window function with a line broadening of 0.3 Hz, and the spectra were phase and baseline corrected using Bruker XWinNMR software (version 3.5).

Identification and quantitation of metabolites

A total of 17 metabolites were identified in the ^{1}H NMR spectra based on their characteristic chemical shifts and multiplicities. Individual metabolite quantities were then calculated by spectral integration of the full resolution data, taking into account the NMR signal intensity and number of protons that contributed to the measured NMR signals for both metabolites and the reference, TSP, and corrected using the total volume of urine excreted in 24 h.

Statistical analysis

Each NMR data set was binned to 4096 points (bin size 0.003 ppm) to minimize the effects of pH and ionic concentration differences. The data were aligned with reference to the TSP

signal, and the regions containing TSP, urea, and residual water (4.6–5.3 ppm) signals were removed. Each NMR data set was then appropriately multiplied using the total 24-h urine volume. The data were mean-centered and divided by the square root of the standard deviation (Pareto scaling) to emphasize both large- and small-concentration metabolite signals. Subsequently, the data were subjected to unsupervised statistical analysis, PCA, using Pirouette software (version 3.11, Infometrix) to classify the samples (control or diabetic). *P* values for the individual metabolites were determined on the actual metabolite quantities using the un-paired t test available in the R software package (http://www.rproject.org). A Benjamini–Hochberg correction was applied to adjust the *P* values by accounting for the 17 metabolites used in the analysis. In addition, the Pearson's correlations among all of the metabolites (for diabetic and control samples separately) were also calculated using R. The statistical significance of the correlation coefficients was tested using a *t* test by giving a null hypothesis (H_0) of $r = 0$, where *r* represents the correlation coefficient. If H_0 holds, $t=\frac{r\sqrt{n-2}}{\sqrt{1-r^2}}$ approximately follows the *t* distribution with degrees of freedom equal to *n*–2, where *n* represents the sample size. A low *P* value (<0.05) for this test means that there is evidence to reject the null hypothesis in favor of the alternative hypothesis or that there is a statistically significant relationship between the two variables (metabolites). Correspondingly, an absolute value of *r* larger than 0.6 (calculated for the control group) or 0.7 (calculated for the diabetic group) is considered as a statistically significant relationship between the two metabolites.

Results

Demographic, blood, and urine parameters

Selected demographic and blood parameters determined by biochemical analysis of diabetic and control rat samples are shown in Table 1. Mean values for plasma glucose, urea, α-tocopherol, TBARS, triglycerides, and liver α-tocopherol were higher in diabetes than control, whereas those for plasma protein and cholesterol were slightly lower. Diabetic rats consumed more water and excreted more than 10 times more urine (mean volume 129 ± 39 ml) than control rats (mean volume 9.6 ± 4.0 ml) in 24 h.

Analysis of NMR spectra

Typical ^{1}H NMR spectra of urine from a diabetic rat and a control rat are shown in Fig. 1 along with the metabolite assignments. Diabetic rat urine spectra contained very high-intensity signals arising from glucose. In addition, the spectra contained numerous signals from the following small molecules: alanine, lactate, ethanol, acetate, pyruvate, 2-oxoglutarate, dimethylglycine, fumarate, succinate, citrate, formate, hippurate, urea, allantoin, dimethylamine, and creatinine. The assignments were made based on literature values [30], and tentative assignments made due to the overlap or slight shift in their positions (such as for glucose, ethanol, pyruvate, fumarate, and allantoin) were confirmed by rerecording ^{1}H NMR spectra for urine before and after the addition of small quantities of the respective standard compounds obtained from commercial sources.

Table 2 shows the metabolite mean quantities and standard deviations in both diabetic and control groups as well as *P* values between the two groups. Glucose excretion was enormous in diabetic rats, with the quantity being nearly 7500-fold higher than in control rats ($P = 0.000099$). The metabolite with the second highest increase was lactate, with the amount being nearly 40-fold higher in diabetes ($P = 0.045$). Other significantly enhanced metabolites were alanine, ethanol, acetate, and fumarate ($P < 0.05$). The average quantities of pyruvate, formate, succinate, and dimethylglycine were 2- to 4-fold higher in diabetes than in controls but were not statistically significant. 2-Oxoglutarate, citrate, hippurate,

allantoin, dimethylamine, and creatinine did not show any large or significant differences (*Ps* = 0.089–0.97).

Multivariate analysis

The PCA scores plot for the quantitative NMR data shows well-separated clusters for disease and control rats (Fig. 2A) and a tight grouping of the control animals. The PC1 loadings plot (Fig. 2B) shows a large number of metabolites in addition to glucose that contributed to the separation. Supervised PLS discriminant analysis also was applied to the data after Pareto scaling and showed similar scores and loadings plots to those for PCA (Fig. S1 in Supplementary material). Although glucose signals dominate the loadings plot, other metabolites such as alanine, lactate, ethanol, acetate, pyruvate, 2-oxoglutarate, dimethylglycine, succinate, formate, and allantoin show positive loadings (similar to glucose). Citrate, creatinine, and hippurate have negative loadings (opposite to glucose). Fumarate does not clearly show up in the PC1 loadings plot, possibly because it has a relatively small variance across all samples as well as a low concentration. The additional contribution of metabolites other than glucose was further demonstrated by performing PCA again (Fig. 2C and D) after removing the glucose region, and the scores plot still shows a clear separation between the diabetic and control rats.

Statistical correlation

To investigate relationships among the metabolites, their quantities were correlated separately for diabetic and control rats using Pearson's correlation (Fig. 3). Correlation coefficients range from 1.0 (maximum positive correlation) to 1.0 (maximum anticorrelation), with a value of 0 representing no correlation. It is clear from the comparison of the two correlation plots in Fig. 3 that the changes between the diabetic and control animals were minimal for the correlation of glucose with alanine, pyruvate, 2-oxoglutarate, fumarate, citrate, allantoin, and creatinine. In diabetic rats, the correlation of glucose with urea was increased dramatically from 0.3 to 1, whereas the correlation of glucose with lactate decreased from 0.6 to 0. The correlation of citrate with alanine, lac-tate, and succinate was decreased from 0.9 to 0.4, from 0.8 to –0.3, and from 0.8 to –0.5, respectively, whereas the correlation of citrate with pyruvate, fumarate, and urea increased. Several metabolites showed a high positive correlation with one another in both diabetes and controls. For example, the metabolite pairs of acetate and ethanol, 2-oxoglutarate and citrate, 2-oxoglutarate and creatinine, and allantoin and creatinine showed high correlation ($R >$ 0.9). Overall, for control rats, most metabolites correlate with one another with high correlation coefficients, as indicated by the predominantly red and orange regions in Fig. 3A, except that acetate, ethanol, and formate are relatively isolated from other metabolites and show blue stripes ($|R| < 0.4$) in the correlation network. In contrast, the increased blue regions in Fig. 3B for the diabetic animals indicate that a number of correlations are significantly decreased and show an overall decrease in metabolic correlation.

Discussion

Upon STZ administration, plasma glucose showed elevated levels, with its quantity being nearly three times higher than in control rats, as anticipated. A number of other changes in blood parameters are also observed (Table 1). However, much more dramatic changes are seen in the urine, as indicated by the ^{1}H NMR data. This is further shown using a quantitative metabolomics approach, in which a distinct classification of diabetic and normal rats is observed (Fig. 2A and B). Statistical analysis of the NMR data, even after removing the glucose signals, showed a number of metabolites contributing to the clear separation of diabetic animals from control animals (Fig. 2C and D). This is corroborated by the high metabolite mean ratios (>2) of 8 of the metabolites (Table 2). As described below, a detailed

analysis of the metabolite correlation matrices (Fig. 3) in combination with their altered metabolite levels indicates a significantly altered metabolism in the glucose metabolism and tricarboxylic acid (TCA) cycles and the effect of gut microbial metabolism in rat diabetes. Fig. 4 compiles these observations based on the KEGG metabolic pathway database (http://www.genome.jp/kegg/pathway.html). Each metabolite is designated using a specific shape and is filled with a specific color to indicate correlations and altered quantities, respectively. Four types of shapes are used to indicate diverse correlations among the observed 17 metabolites, whereas the five different colors are used to indicate the changes in quantities of these metabolites. Three colored borders are used to differentiate the correlations with three key metabolites: glucose (blue), acetate (purple), and creatinine (pink). Black and purple arrows are used to differentiate mammalian pathways from bacterial pathways. The origin and implications of these relationships are discussed below in terms of the altered glucose metabolism, the TCA cycle, and symbiotic metabolism observed in this study.

Endogenous glucose production in the STZ–diabetic rats might be fueled by ingested amino acids along with reduced protein synthesis

Increased glucose in diabetes is due in large part to the enhanced endogenous glucose production (EGP) from noncarbohydrate precursors (gluconeogenesis) and the breakdown of glycogen (glycogenolysis). It has been shown that glycogenolysis was the major factor causing EGP in early stage insulin deficiency [31]. At a later stage, especially for type 1 diabetes, EGP is attributed mainly to gluconeogenesis fueled by amino acids from degraded protein [31] or dietary ingestion. Although such findings are still somewhat in question due to the lack of reliability in the quantitative measurements [32,33], our studies support this hypothesis. In particular, significantly or moderately increased levels of alanine and urea with glucose in diabetes and their increased correlation with one another clearly suggest enhanced amino acids-fueled EGP in diabetes. The increased alanine concentration found in this study for the diabetic rats is in agreement with reports on human type 1 and type 2 diabetes [23,24]. An observed increased correlation of glucose with alanine but not with lactate in diabetic rats suggests that the EGP might be associated more closely with amino acids than with lactate even though the EGP effect from lactate is normally double that arising from alanine [34]. The observations of severely enhanced lactate in both diabetic urine (Table 2) and plasma indicate a significantly reduced consumption of lactate compared with its production. The association of EGP with protein/amino acid metabolism in diabetes was also evident from the observed urea changes. The increased urea average content in both plasma and urine (Tables 1 and 2) in the diabetic animals suggests an increasing nitrogen load to the liver where urea is formed. We observed remarkable changes in the relationship between urea and glucose; there is essentially no correlation between these two metabolites ($R = 0.3$) in the control animals, whereas a strikingly high correlation between glucose and urea ($R = 1.0$) develops in diabetes (Fig. 3). The correlation agrees with a known fact that the amino-acid-fueled EGP enhances the nitrogen load on the liver and, consequently, urea synthesis is closely related to glucose synthesis [35]. Because we observed minimal loss of body mass, the high correlation between urea and glucose in diabetic samples more likely indicates that high glucose is fueled mainly by ingested amino acids along with likely reduced protein synthesis.

Glucose metabolism and TCA cycle were disturbed in the STZ–diabetic rats

A glucose homeostasis was observed in control rats from the positive correlation of glucose with both the gluconeogenesis precursors alanine, lactate, and pyruvate and the TCA cycle intermediates 2-oxoglutarate, fumarate, succinate, and citrate. This can be explained by the fact that a good control of glucose catabolism and anabolism is highly associated with the glucose–alanine and Cori (glucose–lactate) cycles between peripheral tissues and the liver, as demonstrated in Fig. 4. Both lactate and alanine are formed peripherally by glucose-

derived pyruvate and are transported to the liver, where their carbon skeleton is reconverted to glucose. The maintenance of glucose homeostasis also demands a well-functioned TCA cycle capable of producing gluconeogenesis precursors and facilitating glucose oxidation. In addition to the observation that glucose correlates with the identified TCA cycle, it was found from our study that pyruvate (the glycolytic end product that enters the TCA cycle) correlates with the three detected TCA cycle intermediates: 2-oxoglurarate, fumarate, and citrate (Figs. 3A and 4). The metabolic profile from STZ-induced diabetes shows a dramatic perturbation of both glucose metabolism and the TCA cycle, as indicated in both Figs. 3B and 4. First, although glucose correlates highly with alanine, it fails to correlate with lac-tate (Fig. 3B), indicating that the Cori cycle might be perturbed. Second, the correlation of glucose with the TCA intermediates is markedly disturbed with decreasing or missing correlations with 2-oxoglutarate, fumarate, and succinate. Third, the correlations among the TCA intermediates are also significantly altered; for example, succinate no longer correlates with 2-oxoglutarate and citrate in diabetic rats.

Symbiotic metabolism observation 1: A defective acetate switch

An accumulation of acetate in STZ-induced diabetic urine suggests a defective acetate switch, that is, the molecular switch that regulates the dissimilation and assimilation of acetate [36]. The elevation of acetate indicates an increased acetyl–coenzyme A (CoA) pool due to both exogenous (bacterial fermentation) and endogenous (mammalian) production [36,37]. Mammalian up-regulation of acetyl–CoA synthetase 2 (AceCS2) leads to an accumulation of acetate under ketogenic conditions [36]. AceCS2 occurs in most organs but not in the liver, and its up-regulation in other organs stimulates liver excretion of acetate, which accumulates in the bloodstream [36,37]. In addition, the reduced expression of mammalian AceCS1 (which converts acetate to acetyl–CoA) might also contribute partially to acetate accumulation [38].

The observed correlations of acetate with ethanol, lactate, succinate, and formate suggest that the origin of these metabolites may be more microbial than mammalian. It is well known that gut bacteria produce these metabolites, and this evidence was also confirmed by an NMR study of gut fluid (jejunal aspirate) [39]. Another in vitro ^{1}H NMR spectroscopy study on bacteria such as *Klebsiella pneumoniae* showed that the bacteria produced acetate, succinate, and ethanol in the presence of a carbon source such as glycerol [40]. Furthermore, the quantity of these bacterial metabolites increased significantly with increasing bacterial count, establishing their link with the bacteria [39]. The high correlation of acetate with succinate in diabetes ($R = 1$) versus their moderate correlation in controls ($R = 0.6$) is in agreement with the intestinal microbial overgrowth in STZ-induced rats [41]. A strong association between acetate and ethanol was observed in both control and STZ rats. Detection of acetate and ethanol in the rat digestive tract was reported previously [36,42], and their enhancements in diabetes [43,44] are consistent with our results. Alternatively, excess glucose can augment the carbon flux to the TCA cycle, inhibiting the expression of many TCA cycle enzymes and producing a number of partially oxidized metabolites (e.g., ethanol, lactate, formate, succinate). This situation is known as the bacterial Crabtree effect [36]. In the current study, an explanation for the increased amounts of these bacterial metabolites in diabetic rat urine may be due to (i) an increase in bacterial metabolites produced in the gut of diabetic rats due to the microbial overgrowth, (ii) the Crab-tree effect, or (iii) both effects (i) and (ii). Significant levels of bacterial metabolites observed in diabetic rats and their possible origin, gut microbes, could have significant implications for understanding and controlling the secondary effects of these acids on diabetic patients. However, a further investigation is needed to verify this microbial hypothesis.

Symbiotic metabolism observation 2: Altered choline metabolism

Choline is degraded via (i) mammalian pathways in which cho-line is converted to creatinine via dimethylglycine and (ii) symxenobiotic pathways in which choline is converted to methylamine by gut microbiota [45]. A remarkable switch between dimethylglycine and dimethylamine was observed from our study. In controls, dimethylamine correlates highly with glucose, alanine, fumarate, and creatinine, whereas dimethylglycine fails to correlate with these metabolites. In diabetes, on the contrary, dimethyglycine correlates highly with glucose, alanine, fumarate, and creatinine, whereas dimethylamine fails to correlate with these metabolites. The reasons causing such a correlative switch are still unclear at this stage. The significant enhancement of dimethylglycine observed in STZ–diabetic rats may suggest an increased mammalian uptake of dietary choline. Alternatively, an enhanced conversion of choline to dimethylglycine may occur as compared with its conversions to dimethylamine (no observed difference between control and diabetes) or phosphatidylcholine (Fig. 4). The altered choline metabolism could be accounted for by the elevation of plasma triglycerides and liver weight in diabetic rats, as observed from our study (Table 1). High blood glucose levels in the presence of even low insulin levels stimulate the hepatic fatty acid and triglyceride synthesis [46]. Insufficient conversion of choline to phosphatidylcholine exacerbates fatty liver and results in accumulation of triglycerides in plasma [47]. It is possible that the conversion of choline to phosphatidylcholine was reduced due to its potentially enhanced conversion to dimethyglycine in diabetic rats. More studies are required to understand in detail the specific reasons for such a switch in the correlations among the metabolites of the choline pathway.

Accumulation of lactate and pyruvate

Elevation of lactate and pyruvate from the STZ–diabetic rats indicates an increased glycolysis. Because muscle cells in these STZ rats will be glucose starved and would likely oxidize all of the carbon from glucose through oxidative phosphorylation, the high levels of pyruvate and lactate might instead stem from glycolic production of lactate at the level of the red blood cells (RBCs) [48], which express a variant of the enzyme lactate dehydrogenase. It is also possible that other non-insulin-sensitive tissues are metabolizing glucose to lactate, which can be interconverted to pyruvate. This pathway may provide a good compensatory mechanism given that the monocarboxylase transporters, which carry lactate into and out of muscle cells, are not insulin sensitive. Thus, lactate would enter the cell and be converted to pyruvate. However, this scenario does not rule out the possibility of a gut microbial production contribution to the enhanced lactate and pyruvate concentrations. Further investigations need to be carried out to discern the origin of accumulated lactate and pyruvate.

Elevation of TBARS

The TBARS concentration in plasma has been used as an oxidative stress biomarker associated with the presence and amount of final fat degradation products induced by free radicals, and it has been shown to be increased in diabetes and to decrease after treatment with antioxidants [49–52]. This parameter has been highly criticized because of its lack of specificity [53], and although it should not be used alone to reach conclusions, it may add information if used in combination with other oxidative stress biomarkers.

In conclusion, this NMR-based metabolomics approach is useful for the identification and quantitation of high-concentration but important metabolites, and it provides significant information for improving the understanding of disease through the identification of altered metabolic pathways and networks. The urinary metabolites show dramatic changes in this rat diabetic model when compared with blood-based assays. Correlations among the detected metabolites show a number of striking differences between the diabetic and control

rats. Metabolomics-based approaches that identify altered mammalian and symbiotic pathways observed in induced diabetes in rats will be useful for providing additional detailed knowledge concerning metabolic pathways associated with diabetes. Application of these methods to human diabetic patients and a comparison with the derived metabolite and pathway correlations may provide information for identifying additional factors associated with molecular genesis of diabetes and oxidative stress.

Supplementary Material

Refer to Web version on PubMed Central for supplementary material.

Acknowledgments

This work was supported by the National Institutes of Health (NIH) Roadmap Initiative on Metabolomics Technology (Grant NIH/NIDDK 3 R21/R33 DK070290-01), a Collaborative Biomedical Research Grant from Purdue University/Discovery Park, and Spanish MEC project AGL2005-06726-C04-03/ALI. The authors thank Ian R. Lanza for his highly insightful comments.

References

1. Newgard CB, McGarry JD. Metabolic coupling factors in pancreatic beta-cell signal transduction. Annu. Rev. Biochem. 1995; 64:689–719. [PubMed: 7574498]
2. EURODIAB ACE Study Group. Variation and trends in incidence of childhood diabetes in Europe. Lancet. 2000; 355:873–876. [PubMed: 10752702]
3. Jones CW, Reynolds WA, Hoganson GE. Streptozotocin diabetes in the monkey: plasma levels of glucose, insulin, glucagon, and somatostatin, with corresponding morphometric analysis of islet endocrine cells. Diabetes. 1980; 29:536–546. [PubMed: 6103856]
4. Hodavance MS, Ralston SL, Pelczer I. Beyond blood sugar: the potential of NMR-based metabonomics for type 2 human diabetes, and the horse as a possible model. Anal. Bioanal. Chem. 2007; 387:533–537. [PubMed: 17131108]
5. Rossini AA, Like AA, Chick WL, Appel MC, Cahill GF. Studies of Streptozotocin-induced insulitis and diabetes. Proc. Natl. Acad. Sci. USA. 1977; 74:2485–2489. [PubMed: 142253]
6. Sano T, Umeda F, Hashimoto T, Nawata H, Utsumi H. Oxidative stress measurement by in vivo electron spin resonance spectroscopy in rats with streptozotocin-induced diabetes. Diabetologia. 1998; 41:1355–1360. [PubMed: 9833944]
7. Sonta T, Inoguchi T, Tsubouchi H, Sekiguchi N, Kobayashi K, Matsumoto S, Utsumi H, Nawata H. Evidence for contribution of vascular Nad(P)H oxidase to increased oxidative stress in animal models of diabetes and obesity. Free Radic. Biol. Med. 2004; 37:115–123. [PubMed: 15183199]
8. Viant MR, Rosenblum ES, Tjeerdema RS. NMR-based metabolomics: a powerful approach for characterizing the effects of environmental stressors on organism health. Environ. Sci. Technol. 2003; 37:4982–4989. [PubMed: 14620827]
9. Odunsi K, Wollman RM, Ambrosone CB, Hutson A, McCann SE, Tammela J, Geisler JP, Miller G, Sellers T, Cliby W, Qian F, Keitz B, Intengan M, Lele S, Alderfer JL. Detection of epithelial ovarian cancer using ^{1}H NMR-based metabonomics. Int. J. Cancer. 2005; 113:782–788. [PubMed: 15499633]
10. Chen H, Pan Z, Talaty N, Raftery D, Cooks RG. Combining desorption electrospray ionization mass spectrometry and nuclear magnetic resonance for differential metabolomics without sample preparation. Rapid Commun. Mass Spectrom. 2006; 20:1577–1584. [PubMed: 16628593]
11. Pan Z, Raftery D. Comparing and combining NMR spectroscopy and mass spectrometry in metabolomics. Anal. Bioanal. Chem. 2007; 387:525–527. [PubMed: 16955259]
12. Robertson DG. Metabonomics in toxicology: a review. Toxicol. Sci. 2005; 85:809–822. [PubMed: 15689416]
13. Catchpole GS, Beckmann M, Enot DP, Mondhe M, Zywicki B, Taylor J, Hardy N, Smith A, King RD, Kell DB, Fiehn O, Draper J. Hierarchical metabolomics demonstrates substantial

compositional similarity between genetically modified and conventional potato crops. Proc. Natl. Acad. Sci. USA. 2005; 102:14458–14462. [PubMed: 16186495]

14. van der Greef J, Smilde AK. Symbiosis of chemometrics and metabolomics: past, present, and future. J. Chemometr. 2005; 19:376–386.
15. Toye AA, Dumas ME, Blancher C, Rothwell AR, Fearnside JF, Wilder SP, Bihoreau MT, Cloarec O, Azzouzi I, Young S, Barton RH, Holmes E, McCarthy MI, Tatoud R, Nicholson JK, Scott J, Gauguier D. Subtle metabolic and liver gene transcriptional changes underlie diet-induced fatty liver susceptibility in insulin-resistant mice. Diabetologia. 2007; 50:1867–1879. [PubMed: 17618414]
16. Constantinou MA, Papakonstantinou E, Spraul M, Sevastiadou S, Costalos C, Koupparis MA, Shulpis K, Tsantili-Kakoulidou A, Mikros E. ^{1}H NMR-based metabonomics for the diagnosis of inborn errors of metabolism in urine. Anal. Chim. Acta. 2005; 542:169–177.
17. Pan Z, Gu H, Talaty N, Chen H, Shanaiah N, Hainline BE, Cooks RG, Raftery D. Principal component analysis of urine metabolites detected by NMR and DESI–MS in patients with inborn errors of metabolism. Anal. Bioanal. Chem. 2007; 387:539–549. [PubMed: 16821030]
18. Gu H, Chen H, Pan Z, Jackson AU, Talaty N, Xi B, Kissinger C, Duda C, Mann D, Raftery D, Cooks RG. Monitoring diet effects via biofluids and their implications for metabolomics studies. Anal. Chem. 2007; 79:89–97. [PubMed: 17194125]
19. Mortishire-Smith RJ, Skiles GL, Lawrence JW, Spence S, Nicholls AW, Johnson BA, Nicholson JK. Use of metabonomics to identify impaired fatty acid metabolism as the mechanism of a drug-induced toxicity. Chem. Res. Toxicol. 2004; 17:165–173. [PubMed: 14967004]
20. Waters NJ, Waterfield CJ, Farrant RD, Holmes E, Nicholson JK. Integrated metabonomic analysis of bromobenzene-induced hepatotoxicity: novel induction of oxoprolinosis. J. Proteome Res. 2006; 5:1448–1459. [PubMed: 16739996]
21. Wang YL, Holmes E, Tang HR, Lindon JC, Sprenger N, Turini ME, Bergonzelli G, Fay LB, Kochhar S, Nicholson JK. Experimental metabonomic model of dietary variation and stress interactions. J. Proteome Res. 2006; 5:1535–1542. [PubMed: 16823960]
22. Shulman GI. Cellular mechanisms of insulin resistance. J. Clin. Invest. 2000; 106:171–176. [PubMed: 10903330]
23. Zuppi C, Messana I, Tapanainen P, Knip M, Vincenzoni F, Giardina B, Nuutinen M. Proton nuclear magnetic resonance spectral profiles of urine from children and adolescents with type 1 diabetes. Clin. Chem. 2002; 48:660–662. [PubMed: 11901070]
24. Messana I, Forni F, Ferrari F, Rossi C, Giardina B, Zuppi C. Proton nuclear magnetic resonance spectral profiles of urine in type II diabetic patients. Clin. Chem. 1998; 44:1529–1534. [PubMed: 9665433]
25. Salek RM, Maguire ML, Bentley E, Rubtsov DV, Hough T, Cheeseman M, Nunez D, Sweatman BC, Haselden JN, Cox RD, Connor SC, Griffin JL. A metabolomic comparison of urinary changes in type 2 diabetes in mouse, rat, and man. Physiol. Genomics. 2007; 29:99–108. [PubMed: 17190852]
26. Dumas ME, Maibaum EC, Teague C, Ueshima H, Zhou B, Lindon JC, Nicholson JK, Stamler J, Elliott P, Chan Q, Holmes E. Assessment of analytical reproducibility of ^{1}H NMR spectroscopy based metabonomics for large-scale epidemiological research: the INTERMAP study. Anal. Chem. 2006; 78:2199–2208. [PubMed: 16579598]
27. Lindon JC, Holmes E, Nicholson JK. Pattern recognition methods and applications in biomedical magnetic resonance. Prog. Nuclear Magn. Reson. Spectrosc. 2001; 39:1–40.
28. Johnson, RA.; Wichern, DW. Applied Multivariate Statistical Analysis. fifth ed.. Prentice Hall; Upper Saddle River, NJ: 1998.
29. Viana M, Barbas C, Bonet B, Bonet MV, Castro M, Fraile MV, Herrera E. In vitro effects of a flavonoid-rich extract on LDL oxidation. Atherosclerosis. 1996; 123:83–91. [PubMed: 8782839]
30. Lindon JC, Nicholson JK, Everett JR. NMR spectroscopy of biofluids. Annu. Rep. NMR Spectrosc. 1999; 38:1–88.
31. Boden G, Cheung P, Homko C. Effects of acute insulin excess and deficiency on gluconeogenesis and glycogenolysis in type 1 diabetes. Diabetes. 2003; 52:133–137. [PubMed: 12502503]

32. Giaccari A, Morviducci L, Pastore L, Zorretta D, Sbraccia P, Maroccia E, Buongiorno A, Tamburrano G. Relative contribution of glycogenolysis and gluconeogenesis to hepatic glucose production in control and diabetic rats, A re-examination in the presence of euglycaemia. Diabetologia. 1998; 41:307–314. [PubMed: 9541171]
33. Boden G, Chen X, Stein TP. Gluconeogenesis in moderately and severely hyperglycemic patients with type 2 diabetes mellitus. Am. J. Physiol. Endocrinol. Metab. 2001; 280:E23–E30. [PubMed: 11120655]
34. Felig P. The glucose–alanine cycle. Metabolism. 1973; 22:179–207. [PubMed: 4567003]
35. Devlin, MT. Biochemistry with Clinical Correlations. fifth ed.. John Wiley; New York: 2002.
36. Wolfe AJ. The acetate switch. Microbiol. Mol. Biol. Rev. 2005; 69:12–50. [PubMed: 15755952]
37. Buckley BM, Williamson DH. Origins of blood acetate in rat. Biochem. J. 1977; 166:539–545. [PubMed: 597244]
38. Sone H, Shimano H, Sakakura Y, Inoue N, Amemiya-Kudo M, Yahagi N, Osawa M, Suzuki H, Yokoo T, Takahashi A, Iida K, Toyoshima H, Iwama A, Yamada N. Acetyl–coenzyme A synthetase is a lipogenic enzyme controlled by SREBP-1 and energy status. Am. J. Physiol. Endocrinol. Metab. 2002; 282:E222–E230. [PubMed: 11739104]
39. Bala L, Ghoshal UC, Ghoshal U, Tripathi P, Misra A, Gowda GAN, Khetrapal CL. Malabsorption syndrome with and without small intestinal bacterial overgrowth: a study on upper-gut aspirate using ^{1}H NMR spectroscopy. Magn. Reson. Med. 2006; 56:738–744. [PubMed: 16972311]
40. Gupta A, Dwivedi M, Gowda GAN, Mahdi AA, Jain A, Ayyagari A, Roy R, Bhandari M, Khetrapal CL. ^{1}H NMR spectroscopy in the diagnosis of *Klebsiella pneumoniae*-induced urinary tract infection. NMR Biomed. 2006; 19:1055–1061. [PubMed: 16927393]
41. Roza AM, Edmiston CE, Frantzides C, Moore GH, Nowak TV, Johnson CP, Adams MB. Untreated diabetes mellitus promotes intestinal microbial overgrowth. Am. J. Surgery. 1992; 163:417–421.
42. Zumwalt RE, Bost RO, Sunshine I. Evaluation of ethanol concentrations in decomposed bodies. J. Forensic Sci. 1982; 27:549–554. [PubMed: 7119711]
43. Alexander WD, Wills PD, Eldred N. Urinary ethanol and diabetes mellitus. Diabetic Med. 1988; 5:463–464. [PubMed: 2970921]
44. Collison IB. Elevated postmortem ethanol concentrations in an insulin-dependent diabetic. J. Anal. Toxicol. 2005; 29:762–764. [PubMed: 16419416]
45. Dumas ME, Barton RH, Toye A, Cloarec O, Blancher C, Rothwell A, Fearnside J, Tatoud R, Blanc V, Lindon JC, Mitchell SC, Holmes E, McCarthy MI, Scott J, Gauguier D, Nicholson JK. Metabolic profiling reveals a contribution of gut microbiota to fatty liver phenotype in insulin-resistant mice. Prog. Nuclear Magn. Reson. Spectrosc. 2006; 103:12511–12516.
46. Nikkilä EA. Plasma triglycerides in human diabetes. Proc. R. Soc. Med. (Lond.). 1974; 67:662–665.
47. Raubenheimer PJ, Nyirenda MJ, Walker BR. A choline-deficient diet exacerbates fatty liver but attenuates insulin resistance and glucose intolerance in mice fed a high-fat diet. Diabetes. 2006; 55:2015–2020. [PubMed: 16804070]
48. Wiback SJ, Palsson BO. Extreme pathway analysis of human red blood cell metabolism. Biophys. J. 2002; 83:808–818. [PubMed: 12124266]
49. Rupérez FJ, García-Martínez D, Baena B, Maeso N, Cifuentes A, Barbas C, Herrera E. Evolution of oxidative stress parameters and response to oral vitamin E and C administration in streptozotocin diabetic rats. J. Pharm. Pharmacol. 2008; 60:871–878. [PubMed: 18549673]
50. van Dam PS, van Asbeck BS, van Oirschot JF, Biessels GJ, Hamers FP, Marx JJ. Glutathione and alpha-lipoate in diabetic rats: Nerve function, blood flow, and oxidative state. Eur. J. Clin. Invest. 2001; 31:417–424. [PubMed: 11380593]
51. Feillet-Coudray C, Rock E, Coudray C, Grzelkowska K, Azais-Braesco V, Dardevet D, Mazur A. Lipid peroxidation and antioxidant status in experimental diabetes. Clin. Chim. Acta. 1999; 284:31–43. [PubMed: 10437641]
52. Baydas G, Canatan H, Turkoglu A. Comparative analysis of the protective effects of melatonin and vitamin E on streptozotocin-induced diabetes mellitus. J. Pineal Res. 2002; 32:225–230. [PubMed: 11982791]

53. Verhagen H, Aruoma OI, van Delft JH, Dragsted LO, Ferguson LR, Knasmüller S, Pool-Zobel BL, Poulsen HE, Williamson G, Yannai S. The 10 basic requirements for a scientific paper reporting antioxidant, antimutagenic, or anticarcinogenic potential of test substances in in vitro experiments and animal studies in vivo. Food Chem. Toxicol. 2003; 41:603–610. [PubMed: 12659712]

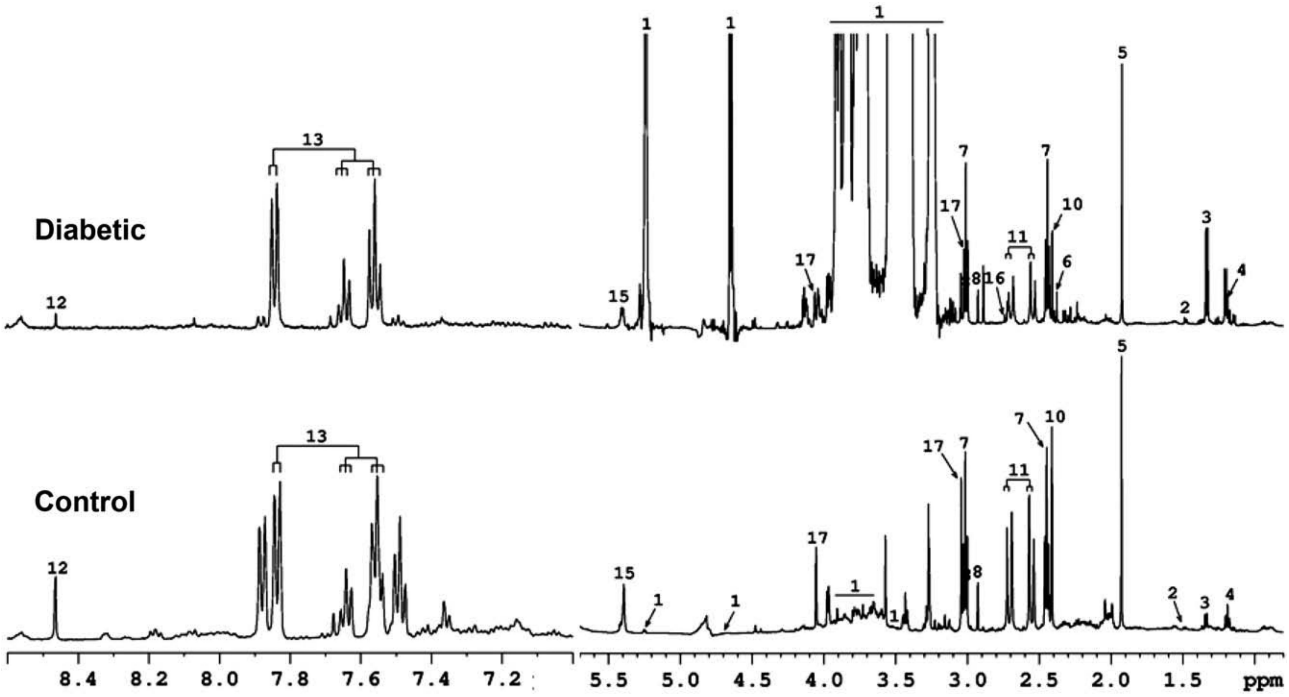

Fig. 1.

Typical ^{1}H NMR spectra of urine from a Sprague–Dawley control rat and an STZ-induced diabetic rat. Identified metabolites: 1, glucose; 2, alanine; 3, lactate; 4, ethanol; 5, acetate; 6, pyruvate; 7, 2-oxoglutarate; 8, dimethylglycine; 9, fumarate; 10, succinate; 11, citrate; 12, formate; 13, hippurate; 14, urea; 15, allantoin; 16, dimethylamine; 17, creatinine.

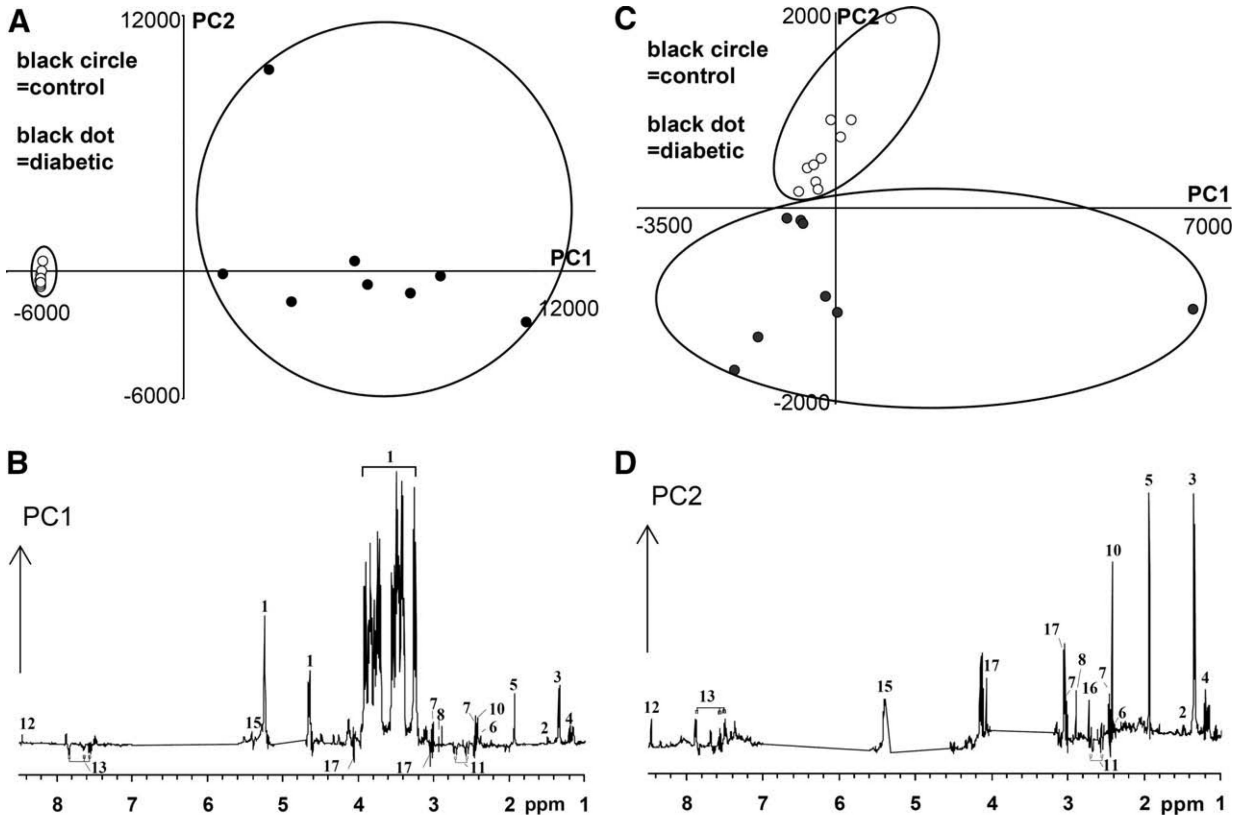

Fig. 2.

(A and B) Scores plot (A) and PC1 loadings plot (B) from the PCA of ^{1}H NMR spectra of urine from diabetic and control rats (urea and residual water peaks were removed prior to PCA). (C and D) Scores plot (C) and PC2 loadings plot (D) from the PCA of ^{1}H NMR spectra of urine from diabetic and control rats (glucose, urea, and residual water peaks were removed prior to PCA). Intensities of the NMR variables were scaled using the total volume of urine collected over 24 h. The data were analyzed after applying Pareto scaling.

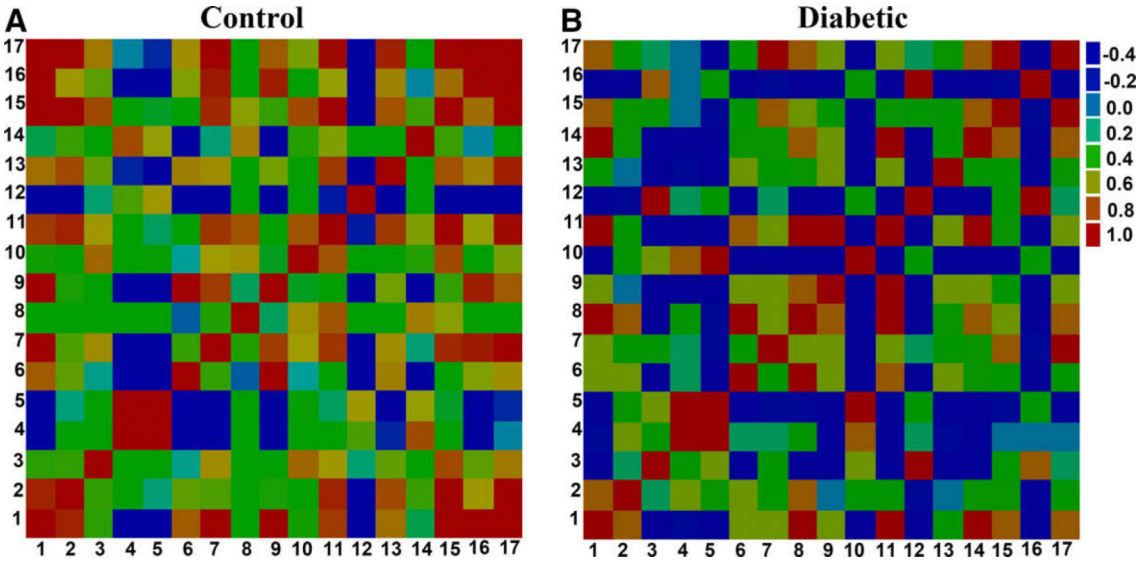

Fig. 3.

Pearson's correlations of the quantities of the 17 metabolites determined from rat urine samples: (A) control; (B) diabetic. The numbers for the metabolites used are as given in Table 2. (For interpretation of the references to color in the description of this figure in the text, the reader is referred to the Web version of this article.)

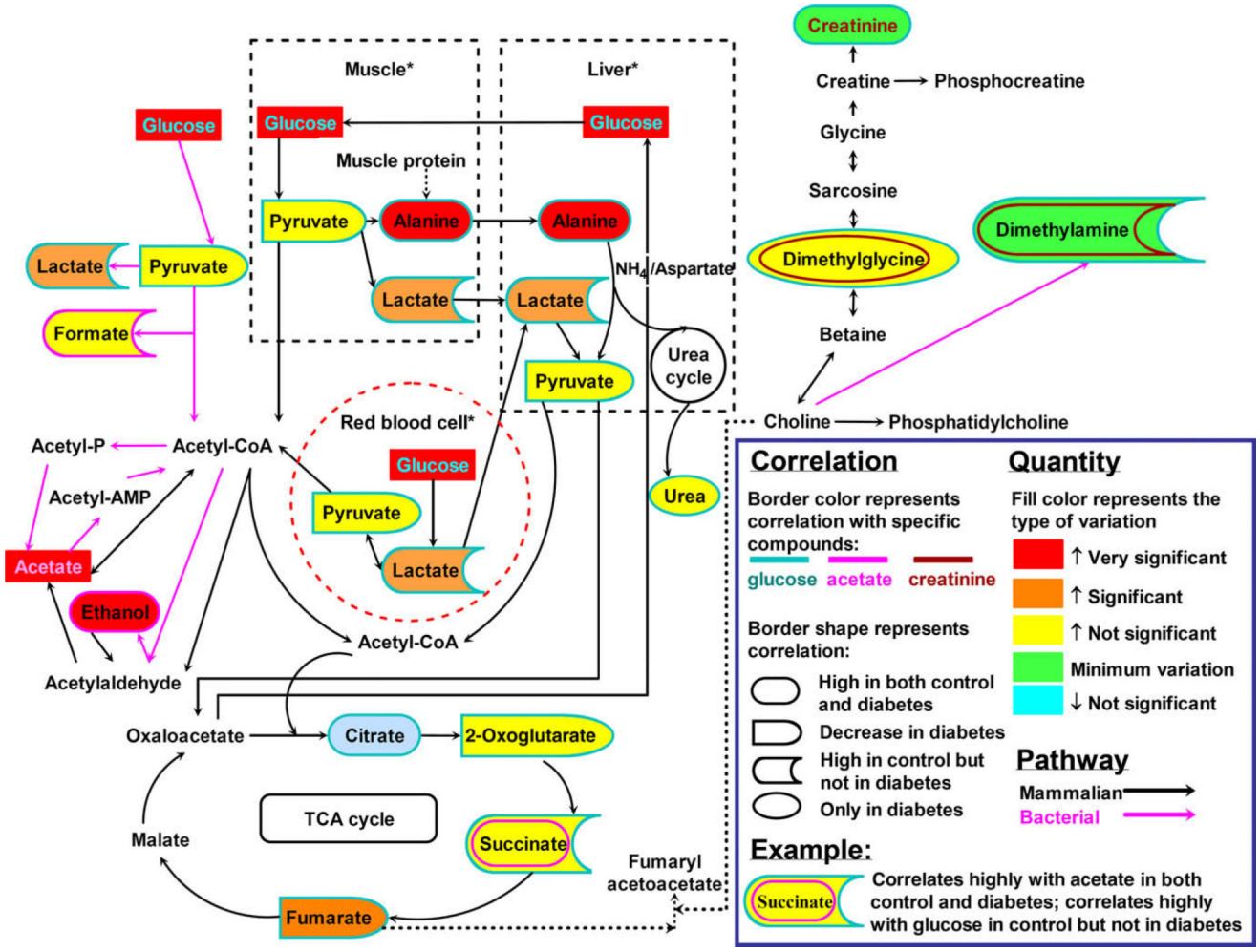

Fig. 4.

Schematic diagram of the disturbed metabolic pathways detected by ^{1}H NMR urine analysis. *Tissue compartments are used to illustrate the glucose–alanine and Cori cycles. (For interpretation of the references to color in this figure and in the description of the figure in the text, the reader is referred to the Web version of this article.)

Table 1

Demographic and blood biochemical parameters for STZ-induced diabetic and control rats

Parameter	Control rats (*n* = 18)	Diabetic rats (*n* = 22)
Weight (g)	241 ±5	239 ± 6
Plasma glucose (mmol/L)	9.87 ± 0.54	31.30 ± 7.70
Plasma α-tocopherol (μmol/L)	25.4 ± 1.2	43.2 ± 12.8
Plasma urea (mmol/L)	6.49 ± 0.72	8.14 ± 2.05
Plasma triglycerides (mmol/L)	0.71 ± 0.06	5.21 ± 2.60
Plasma protein (g/L)	0.056 ± 0.001	0.052 ± 0.003
Plasma cholesterol (mmol/L)	2.32 ± 0.09	2.29 ± 0.26
Plasma TBARS (μmol/L)	90.2 ± 6.9	160 ± 62
Liver α-tocopherol (μg/g)	28.9 ± 2.3	45.7 ± 10.2
Liver weight (g)	8.2 ± 0.2	8.7 ± 0.8
Urine volume (24 h) (ml)	9.59 ± 3.96	129 ± 39

Note. Results are from a larger number of rats spanning several studies but treated in the same manner as described in the text.

Table 2

Quantitative comparison of 17 metabolites found in diabetic and control rat urine

Identification number	Metabolite	Control rats[a] (mol/24 h)	Diabetic rats[a] (mol/24 h)	*P* value[b]
1	Glucose	8.5 ± 8.7	61,800 ± 21,800	0.0000099
2	Alanine	1.6 ± 1.0	7.0 ± 2.4	0.00015
3	Lactate	5.6 ± 4.8	245 ± 262	0.045
4	Ethanol	6.9 ± 6.4	46.6 ± 33.3	0.027
5	Acetate	41.2 ± 38.8	192 ± 132	0.037
6	Pyruvate	2.2 ± 1.9	8.2 ± 7.9	0.065
7	2-Oxoglutarate	100 ± 9	163 ± 97	0.089
8	Dimethylglycine	5.1 ± 2.9	10.5 ± 5.5	0.23
9	Fumarate	1.8 ± 1.5	2.3 ± 0.6	0.045
10	Succinate	28.8 ± 17.0	76.5 ± 67.5	0.11
11	Citrate	75.8 ± 39.8	51.7 ± 42.2	0.42
12	Formate	4.6 ± 6.2	10.0 ± 12.4	0.61
13	Hippurate	35.3 ± 17.8	32.6 ± 29.8	0.97
14	Urea	6.8 ± 3.6	9.6 ± 3.3	0.58
15	Allantoin	39.3 ± 21.7	42.9 ± 14.0	0.61
16	Dimethylamine	5.5 ± 3.1	5.8 ± 5.9	0.71
17	Creatinine	41.1 ± 25.4	33.6 ± 14.1	0.83

[a] The quantities were determined from ^{1}H NMR analysis of 24-h urine from diabetic and control rats.

[b] Unpaired *t* test using a Benjamini–Hochberg correction to the *P* values.